arXiv:cond-mat/0603200v1 [cond-mat.mes-hall] 8 Mar 2006

Ordered structures in rotating ultracold Bose gases

N. Barberán[1], M. Lewenstein[2,3], K. Osterloh[3], and D. Dagnino[1]

[1]*Dept. ECM, Facultat de Física, U. de Barcelona, E-08028 Barcelona, Spain*

[2]*ICREA and ICFO–Institut de Ciències Fotòniques,*

Av. del Canal Olímpico s/n, 08860 Castelldefells, Barcelona, Spain and

[3]*Institute for Theoretical Physics, University of Hannover,*

Appelstrasse 2, 30167 Hannover, Germany

Abstract

The characterization of small samples of cold bosonic atoms in rotating microtraps has recently attracted increasing interest due to the possibility to deal with a few number of particles per site in optical lattices. In this paper we consider two-dimensional systems of few cold Bose atoms confined in a harmonic trap in the XY plane, and submitted to strong rotation around the Z axis. By means of exact diagonalization, we analyze the evolution of ground state structures as the rotational frequency Ω increases. Various kinds of ordered structures are observed. In some cases, hidden interference patterns exhibit themselves only in the pair correlation function; in some other cases explicit broken-symmetry structures appear that modulate the density. For $N < 10$ atoms, the standard scenario, valid for large sytems (i.e. nucleation of vortices into an Abrikosov lattice, melting of the lattice, and subsequent appearance of fractional quantum Hall type states up to the Laughlin state), is absent for small systems, and only gradually recovered as N increases. On the one hand, the Laughlin state in the strong rotational regime contains ordered structures much more similar to a Wigner crystal, or a molecule than to a fermionic quantum liquid. This result has some similarities to electronic systems, extensively analyzed previously. On the other hand, in the weak rotational regime, the possibility to obtain equilibrium states, whose density reveals an array of vortices, is restricted to some critical values of the rotational frequency Ω. The vortex contribution to the total angular momentum L as a function of Ω ceases to be an increasing function of Ω, as observed in experiments of Chevy *et al.* [1]. Instead, for small N, it exhibits a sequence of peaks showing wide minima at the values of Ω, where no vortices appear.

PACS numbers: 73.43.-f, 05.30.Jp, 03.75.Kk

Keywords: Strongly rotating Bose gas. Symmetry broken states. Exact diagonalization.

I. INTRODUCTION

A. Ordered structures in ultracold gases and their detection

Ordered structures, and in particular hidden ordered structures have been a subject of intensive studies in the physics of Bose-Einstein condensates (BEC's) [2, 3, 4, 5], and more generally, in the physics of ultracold atoms.

The paradigm example of such structures is realized in the interference of two BEC's, observed in seminal experiments of Ref. [6]. Suppose that, despite the superselection rule, one could prepare the two condensates in coherent atomic states, characterized by fluctuating atom numbers N_1, N_2, but sharply defined phases ϕ_1, ϕ_2, minimizing the Heisenberg uncertainty relation for the number and phase operators. Then, the phase difference $\Delta\phi = \phi_1 - \phi_2$ would determine the position of the interference fringes. Similarly, if we prepared two condensates by, say, splitting a parent condensate with fixed number of atoms $N = N_1 + N_2$, we would arrive at sharp values of both $\Delta\phi$ and $N_1 - N_2$. Amazingly, the interference pattern will also appear if the two BEC's in the Fock states (with fixed N_1 and N_2) overlap. The reason is, as pointed out in Ref. [7, 8], that as soon as we start detecting atoms without knowing which condensate they originate from, the measurement will introduce the necessary uncertainty of the atom numbers, narrowing the relative phase distribution. As a consequence, an interference pattern with a sharply defined $\Delta\phi$ is obtained in each realization of the measurement. We may say that the measurement process uncovers the otherwise hidden interference pattern in the two-point first order correlation function of atomic creation and annihilation field operators, $\langle\hat{\Psi}^\dagger(\mathbf{r})\hat{\Psi}(\mathbf{r}')\rangle$. If experimentally averaged over many realizations the interference pattern vanishes, since each realization leads to a different and completely random $\Delta\phi$. Similar measurement induced structures, and the interplay between single shot and averaged results have also been discussed in the context of dark solitons in BEC [9].

Other types of ordered structures occur in rotating BEC's. In the standard scenario, as the rotational frequency increases, more and more vortices appear in form of regular structures [5, 10, 11]. As their number grows, they organize themselves in a triangular Abrikosov lattice [12]. Note, that in principle the ground state of the rotating system in a harmonic trap should ideally be rotationally invariant and have a fixed total angular

momentum L, *ergo* it should not exhibit any structures that break rotational symmetry, as the Abrikosov lattice does. In reality though, the preparation of vortices is performed by a "laser stirring" process that breaks rotational symmetry, and introduces significant couplings between states with different total angular momenta [13]. Here, one deals with a situation in which the preparation process (which may also be regarded as a form of measurement) reveals elsewise hidden structures in the density of the condensate, i.e., in the one-point first order correlation function $\langle\hat{\Psi}^\dagger(\mathbf{r})\hat{\Psi}(\mathbf{r})\rangle$.

As it is very well known from quantum optics, measurements of first order correlation functions (first order "coherence") do not always reveal the underlying structures. In order to see them, one has to measure higher order coherences, such as second order correlation functions $\langle\hat{\Psi}^\dagger(\mathbf{r}_1)\hat{\Psi}^\dagger(\mathbf{r}_2)\hat{\Psi}(\mathbf{r}_3)\hat{\Psi}(\mathbf{r}_4)\rangle$. The paradigm example for this necessity goes back to Michelson interferometry [14] which measures first order coherences and is sensitive to atmospheric fluctuations. This deficiency of Michelson interferometry has stimulated Hanbury Brown and Twiss [15] to measure the intensity-intensity correlations of the radiation coming from Sirius, which in turn allowed them to precisely determine the coherence length and the angular size of this star.

Measurements of second order correlations play an important role in the physics of ultracold gases (for earlier works on atomic beams, see [16]). The most directly measurable quantity is the density-density correlation (pair correlation function, called pc function below): $\langle\hat{\Psi}^\dagger(\mathbf{r}_1)\hat{\Psi}^\dagger(\mathbf{r}_2)\hat{\Psi}(\mathbf{r}_2)\hat{\Psi}(\mathbf{r}_1)\rangle$, which formally is the two-point second order correlation function of the atomic field operators. This function has been directly measured in a recent atom counting experiment of the Orsay group [17], for the first time directly demonstrating an atomic Hanbury Brown-Twiss effect for thermal atoms and the second order coherence of a BEC. Earlier, a 4-point second order correlation function has been measured in Hannover [18] where density-density correlations of *interfering condensates* have been monitored in order to precisely determine the phase coherence length of quasi-1D condensates, in full analogy to the Hanbury Brown and Twiss method.

Recently, yet another tool, i.e., *noise interferometry* has been proposed to analyze visible and hidden structures appearing in various quantum phases of ultracold gases [19, 20]. This method also allows to determine density-density correlations, and has been used by several groups to study, for instance, interference of independent BEC's [21], residual coherence

and lattice order in Mott insulators [22], and pair correlations of fermionic atoms in a Fermi superfluid [23].

At this point it is necessary to mention that the double (spatial and temporal) Fourier transform of the pc function is known to be a dynamical structure factor [5], and is also measurable, for instance in Bragg scattering experiments [24].

B. Rapidly rotating ultracold gases

Recently, a considerable interest has been devoted to rapidly rotating ultracold gases, which also exhibit various kinds of ordered structures, and should therefore be investigated along the lines discussed in the previous subsection.

Typically, one considers a quasi 2D gas in the XY plane rotating around the Z axis with frequency Ω, and confined in a harmonic trap of frequency $\omega_\perp$. As stated above, in macroscopic atomic clouds for moderate $\Omega < \omega_\perp$, the Abrikosov vortex lattice is formed [10, 11]. As Ω approaches $\omega_\perp$, the vortex lattice melts, and the system evolves through a sequence of strongly correlated states [26, 27]. Finally, in the regime of critical rotation, it forms a bosonic Laughlin liquid [25].

Alternatively, the various regimes of rapidly rotating gases can be described in the terminology of fractional quantum Hall effect (FQHE) theory [28]. The crucial role is played by the direct analog of the Landau level filling factor in the FQHE which can be related to the number of vortices N_v by $\nu = N/N_v$ as defined in the BEC mean field description valid for large systems and moderate rotation.

The first papers on atomic systems [26, 27] have considered the lowest Landau level (LLL) for strong enough rotation. Recently, correlated liquids at $\nu = k/2$ for $k = 1, 2, 3, \ldots$ for $\nu \leq \nu_c \simeq 6 - 10$ have been discussed [29]. These states resemble to a great extent the states from the Rezayi-Read (RR) hierarchy [30]: $k = 1$ is the Laughlin state, $k = 2$ is the Moore-Read paired state [31] etc. It has been shown that the presence of but a small amount of dipole-dipole interactions unambiguously makes the RR state with $k = 3$ the ground state at filling $\nu = 3/2$. This state is particularly interesting, since its excitations are both fractional and non-Abelian. The validity of the LLL approximation for rotating gases is also discussed in the recent preprint [32].

Most of the literature on ultracold rapidly rotating gases aims at considering relatively large systems and even the thermodynamic limit. In numerical simulations, either periodic (torus) or spherical boundary conditions are used. Unfortunately, in the $N \to \infty$ limit the gap separating the Laughlin state from its excitations vanishes. Observation of Laughlin states not only requires to reach the LLL, but also to control very precisely a delicate balance between Ω and $\omega_\perp$. Despite the progress in experimental studies of vortex lattices [33, 34], and first steps towards LLL physics [35], experiments have not yet reached this regime.

The problems related to the short range nature of the Van der Waals forces can be overcome in dipolar gases, i.e. gases that interact via magnetic or electric dipole moments (for a review see [36]). Rotating dipolar bosonic gases are expected to exhibit exotic behaviour in the weakly interacting regime [37], whereas fermionic dipolar gases have a finite gap for the $\nu = 1/3$ Laughlin state [38]. The first observation of BEC of a dipolar gas of Chromium atoms with large magnetic dipole has been recently reported [39], and several groups are trying to realize and control an ultracold gas of heteronuclear molecules with large electric dipole moments [40].

Another way to create highly-correlated liquids could be, not to mimic effects of magnetic fields by rotation, but by appropriately designed control of tunnelling phases in optical lattices [41]. In trapped gases, a similar effect may be realized by employing electromagnetically induced transparency [42].

However, the most promising way towards the FQH regime and related states may be achieved by use of an array of rotating optical microtraps, either in an optical lattice [43], or created by an array of rotating microlenses [44].

In such arrangements, it will be natural to study mesoscopic, or even microscopic systems of few atoms. Such experiments demand careful theoretical studies of few atom systems using possibly exact methods, such as exact diagonalizations of the Hamiltonian with open boundary conditions in the presence of the harmonic trap, or even a deformed trap. Such studies have recently been initiated [45], and the possibilities of an adiabatic path to fractional quantum Hall states of a few bosonic atoms have been investigated in detail. We continue the studies of small systems of atoms in rotating traps, and expand them in the present paper.

C. Plan of the paper

The main focus of the present paper is to study and analyze the ground state (GS) ordered structures and interference patterns (IP) of two-dimensional Bose systems of few atoms confined in a harmonic trap and submitted to fast rotation around the perpendicular axis. We investigate here, on one hand, the situations where the cylindrical symmetry is explicitly broken so that the one particle density already exhibits ordered structures due to the coherent mixing of degenerated GS with different total angular momenta. Furthermore, we consider situations in which the ordered patterns are hidden in a pure single state with well defined angular momentum, and are evident only through inspection of the pair correlation (pc) function calculated by means of exact diagonalization. This formalism turns out to be the appropriate method to deal with small systems, for which the assumptions made in mean field theories do not apply. Such systems are experimentally accessible, and both, density and pc functions, are measurable by various experimental techniques discussed in the previous subsection. Experimental information on the IP can be obtained in the last case.

According to our findings, the behaviour of confined systems of few atoms strongly differs from the behaviour of large systems. These differences are not only related to the nucleation of vortices in the regime of relatively slow rotation, but also to the nature of the Laughlin state and other highly-correlated states, when the rotational frequency is close to the trap frequency.

In particular, we obtain that for $N < 10$ atoms the standard scenario valid for large sytems (i.e., the nucleation of vortices into an Abrikosov lattice, melting of the lattice, and subsequent appearance of fractional quantum Hall type states up to the Lauhglin state), is absent for small systems, and is only gradually recovered as N increases. On the one hand, the Laughlin state in the strong rotational regime contains ordered structures much more similar to a Wigner crystal or a molecule than to a Fermi liquid. This result has some similarities to electronic systems, extensively analyzed previously. On the other hand, in the weak rotational regime, the possibility to obtain equilibrium states whose density reveals an array of vortices is restricted to some critical values of the rotation frequency Ω. The vortex contribution to the total angular momentum L as a function of Ω ceases to be an increasing function of Ω, as observed in experiments of Chevy *et al.* [1]. Instead, for small

N, it exhibits a sequence of peaks showing wide minima at the values of Ω, where no vortices appear.

This paper is organized as follows. In Sec. II we describe our system (Section IIA) and address the questions related to the realization and analysis of ground states with hidden (Section IIB), or explicit (Section IIC) broken cylindrical symmetry. In Sec. III, the main results of this work are presented. Finally, in Sec. IV, we compare our findings with previous results in the literature, and draw our conclusions.

II. ORDERED STRUCTURES IN GROUND STATES: BROKEN CYLINDRICAL SYMMETRY

A. Description of the system

Our system consists of N bosonic atoms trapped in a rotating parabolic potential. The Hamiltonian in the rotating reference frame reads [46],

$$H = \sum_{i=1}^{N} \left[\frac{(\vec{p} - \frac{e}{c}\vec{A}^*)_i^2}{2M} + \frac{1}{2} M(\omega_\perp^2 - \Omega^2) r_i^2 \right] + g \sum_{i<j} \delta(\vec{r}_i - \vec{r}_j), \tag{1}$$

where $\vec{r} = (x, y)$, $\omega_\perp$ is the trap frequency, $\vec{A}^* = \frac{M\Omega c}{e} \hat{z} \times \vec{r}$ is the vector potential, $\hat{z}$ is the unitary vector along the Z direction and $\vec{B}^* = \vec{\nabla} \times \vec{A}^* = \frac{2M\Omega c}{e} \hat{z}$ is the effective magnetic field of an equivalent system of electrons submitted to a magnetic field perpendicular to the XY plane (we use here the symmetric gauge). Thus, the rotation of the trap has formally the same effect on atoms of mass M, as a magnetic field has on electrons; the electronic charge $-e$ and the speed of light c are solely introduced for reasons of algebraic equivalence. $V = g \sum_{i<j} \delta(\vec{r}_i - \vec{r}_j)$ is the contact interaction potential, where g is the interaction coefficient that approximates the potential of the Van der Waals forces between the atoms in the very dilute limit. We assume the rotational frequency to be large enough to restrict the system to the lowest Landau level (LLL) regime, and choose the appropriate Fock–Darwin single particle (sp) wave functions with no nodes in the radial direction, as the basis in order to represent all operators [47],

$$| \, m\rangle = \frac{1}{\lambda\sqrt{\pi m!}} \left(\frac{z}{\lambda}\right)^m e^{-|z|^2/2\lambda^2} \tag{2}$$

with $\lambda = \sqrt{\frac{\hbar}{2M\omega_\perp}}$, and generalized complex coordinates $z = x + iy$.

The Hamiltonian can be written in second quantized form as,

$$\hat{H} = \alpha \hat{L} + \beta \hat{N} + \hat{V}, \tag{3}$$

where $\alpha = \hbar(\omega_\perp - \Omega)$, $\beta = \hbar\omega_\perp$, $\hat{L}$ and $\hat{N}$ are the total z-component angular momentum and particle number operators, respectively, and

$$\hat{V} = \frac{1}{2} \sum_{m_1 m_2 m_3 m_4} V_{1234} \;\; a_1^\dagger a_2^\dagger a_4 \, a_3 \quad , \tag{4}$$

where the matrix elements of the interaction term are given by

$$V_{1234} = \langle m_1 \, m_2 \mid V \mid m_3 \, m_4 \rangle = \frac{g}{\lambda^2 \pi} \; \frac{\delta_{m_1+m_2, m_3+m_4}}{\sqrt{m_1! m_2! m_3! m_4!}} \; \frac{(m_1+m_2)!}{2^{m_1+m_2+1}} \; . \tag{5}$$

Here, the operators $a_i^\dagger$ and a_i create and annihilate a boson with single-particle (sp) angular momentum m_i, respectively. The cylindrical symmetry of the Hamiltonian allows the diagonalization to be performed in different subspaces of well defined total z-component of angular momentum $L = \sum_{i=1}^N m_i$.

Fig. 1 shows the total angular momentum of the GS of a system of $N = 5$ particles while Ω grows from zero to $\omega_\perp$, the maximum possible value before the system becomes centrifugally unstable. We observe that the GS angular momentum remains constant for a finite range of Ω until transitions to new angular momenta take place at critical values labelled as Ω_{cn}. Not all L-values can be associated with the GS's. However, on the steps, different L-states may be degenerate in energy as in the case of the states with $L = 8, 10$ and 12 on the third step (indicated by stars in Fig. 1). The last possible GS at $L = N(N-1)$ is the Laughlin state, for which the interaction energy is zero due to the fact that the wave function of each atom has zeros of order two at the positions of the other $N-1$ atoms; this can be easily deduced from the analytical expression of the many-body wave function given by,

$$\Psi_{Laughlin} = \mathcal{N} \prod_{i<j} (z_i - z_j)^2 e^{-\sum |z_i|^2 / 2\lambda^2} \quad . \tag{6}$$

In the following, the GS of the system in the L-subspace is denoted by Ψ_L. In order to study the nature of the GS's, it is useful to analyze the expectation values of some relevant

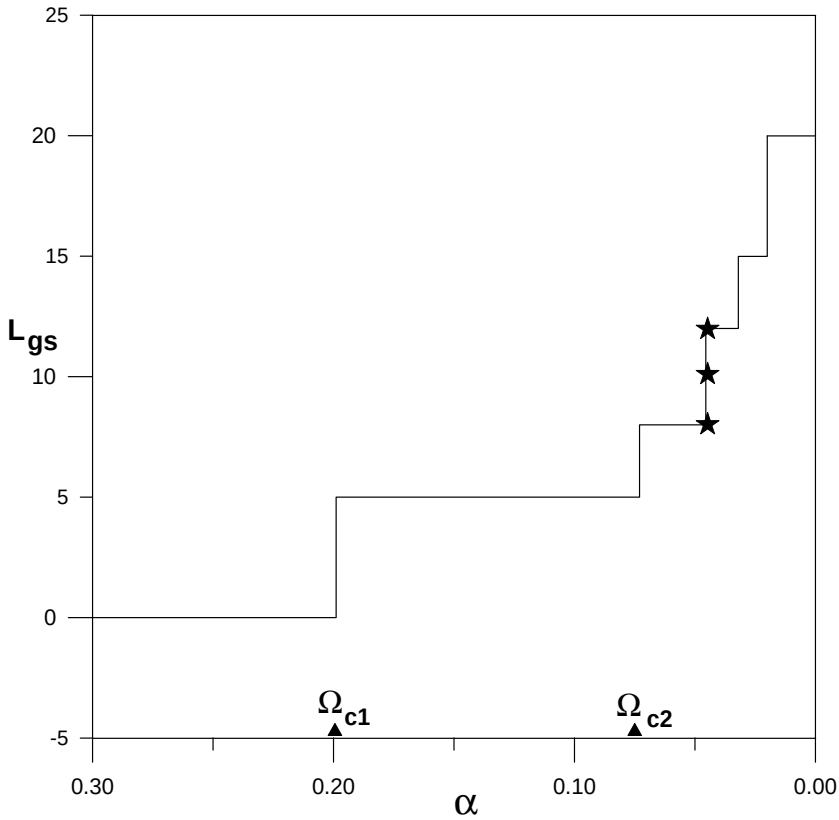

FIG. 1: Change of the GS angular momentum L_{gs} for $N = 5$ as the rotation frequency increases; transitions take place at critical values of the rotational frequency labelled by Ω_{cn}. ($\alpha = \hbar(\omega_\perp - \Omega)$).

operators. First of all, it is crucial to realize that the density operator defined in first quantization as

$$\hat{\rho}(\vec{r}) = \sum_{i=1}^{N} \delta(\vec{r} - \vec{r}_i) \tag{7}$$

does not exhibit any interference pattern when calculated for a definite Ψ_L, as it can be inferred from its analytical expression in second quantized form

$$\hat{\rho}(\vec{r}) = \sum_{ij} \langle \phi_i(\vec{r'}) \mid \delta(\vec{r} - \vec{r'}) \mid \phi_j(\vec{r'}) \rangle a_i^\dagger a_j, \tag{8}$$

where $|\phi_i(\vec{r})\rangle = |m_i\rangle$ as in Eq. (2). Due to angular momentum conservation, the operator $a_i^\dagger a_j$ selects only one sp state and, as a consequence, it loses all information contained in products of different amplitudes, thus losing the interference pattern. It solely preserves the information of individual densities, e.g.,

$$\rho(\vec{r}) = \langle \Psi_L \mid \hat{\rho}(\vec{r}) \mid \Psi_L \rangle = \sum_{i}^{N} \mid \phi_i(\vec{r}) \mid^2 Oc_i \ , \tag{9}$$

where Oc_i is the total occupation of the sp state $|m_i\rangle$ in the GS. In effect, $\rho(\vec{r})$ can only represent cylindrically symmetric distributions. However, we note that this cylindrical symmetry is a direct consequence of the definition of the operator $\hat{\rho}(\vec{r})$, and is not necessarily a manifestation of the symmetric nature of the GS.

To exhibit ordered patterns and analyze the GS structures, we proceed in two different ways; one investigates the pair correlation function for states with fixed L (Section IIB), the other combines different Ψ_L's (Section IIC).

B. Ordered structures in pair correlation functions

In order to analyze the internal structure of relevant states, we consider the following operator

$$\hat{\rho}(\vec{r},\vec{r}_0) = \sum_{i<j}^{N} \delta(\vec{r}_i - \vec{r}_0)\delta(\vec{r}_j - \vec{r}), \tag{10}$$

which yields the conditional probability to find an atom at $\vec{r}$, when another is simultaneously found at $\vec{r}_0$. This operator contains information that originates from the amplitudes of sp wave functions, and not only from their density as it has been in case of the single particle density operator. In second quatized formalism, its expected value with respect to Ψ_L reads

$$\rho(\vec{r},\vec{r}_0) = \sum_{ijkl}\sum_{pp'} \alpha_p^* \alpha_{p'} \phi_i^*(\vec{r})\phi_j^*(\vec{r}_0)\phi_k(\vec{r})\phi_l(\vec{r}_0)\langle \Phi_p \mid a_i^\dagger a_j^\dagger a_l a_k \mid \Phi_{p'}\rangle, \tag{11}$$

where

$$\Psi_L = \sum_{p=1}^{n_d} \alpha_p \Phi_p, \tag{12}$$

and Φ_p are the bosonic Fock N-body states of the basis in the L-subspace of dimension n_d. The condition $i+j=k+l$ must be fulfilled for reasons of angular momentum conservation. It should be stressed that $\rho(\vec{r},\vec{r}_0)$ in Eq. (10) obviously differs from the single particle density matrix

$$n^{(1)}(\vec{r},\vec{r'}) = \langle \hat{\Psi}^+(\vec{r})\hat{\Psi}(\vec{r'})\rangle, \tag{13}$$

which defines the off-diagonal long-range order that characterizes Bose condensation [5]. The operator $\hat{\rho}$ is a two-particle operator, whereas $\hat{n}^{(1)}(\vec{r},\vec{r'}) = \hat{\Psi}^+(\vec{r})\hat{\Psi}(\vec{r'})$ is a single-particle operator; in particular, $\rho(\vec{r}) = n^{(1)}(\vec{r},\vec{r})$, whereas $\rho(\vec{r}) = \frac{1}{N-1}\int d\vec{r}_0 \rho(\vec{r},\vec{r}_0)$. As a

rule of thumb, if $\hat{n}^{(1)}(\vec{r},\vec{r'})$ reveals symmetry breaking, so does $\hat{\rho}$, whereas the opposite is not necessarily true.

Eq. (11) can be interpreted as the sum of products of amplitudes at $\vec{r}$ weighted by a factor that depends on $\vec{r}_0$, and on the GS via the α_p coefficients. In the particular case $\vec{r}_0 = \vec{0}$, cylindrical symmetry is recovered, since in this case $l = j = 0$ is the unique non-zero contribution. This implies $i = k$ and yields

$$\rho(\vec{r},\vec{0}) =\mid \phi_0(\vec{0}) \mid^2 \sum_i \mid \phi_i(\vec{r}) \mid^2 \sum_{pp'} \alpha_p^* \alpha_{p'} \langle ... \rangle, \tag{14}$$

which is independent from θ.

In order to understand the role of the parameter $\vec{r}_0$ in $\langle \Psi_L \mid \hat{\rho}(\vec{r},\vec{r}_0) \mid \Psi_L \rangle$ as a function of $\vec{r}$, we consider

$$\phi_n^*(\vec{r})\phi_j^*(\vec{r}_0)\phi_k(\vec{r})\phi_l(\vec{r}_0) = \frac{1}{\pi^2}\frac{r^{m_n}}{\sqrt{m_n!}}\frac{r_0^{m_j}}{\sqrt{m_j!}}\frac{r^{m_k}}{\sqrt{m_k!}}\frac{r_0^{m_l}}{\sqrt{m_l!}} e^{i(m_k-m_n)\theta} e^{i(m_l-m_j)\theta_0} e^{-r^2} e^{-r_0^2}, \tag{15}$$

in units of λ. As $l - j = n - k$ follows from angular momentum conservation, the angular dependence reads

$$e^{i(m_k-m_n)\theta} e^{i(m_l-m_j)\theta_0} = e^{i(m_k-m_n)(\theta-\theta_0)}. \tag{16}$$

Evidently, if r_0 is fixed, the change of θ_0 is nothing but a rigid rotation of the function. In other words, any arbitrary choice of θ_0 fixes the origin of angles, and breaks cylindrical symmetry, in the analogous way as it happens in experiments which perform a single shot measurement. Within this point of view, the experimental measurement and the choice of θ_0 are equivalent processes (see for instance [19, 22]).

The expected values of the pc function for $r_0 \neq 0$ can reveal very different situations: from circular symmetric structures showing no spatial correlation, to ordered structures that reveal intrinsic Wigner molecules or crystals while passing through all possible intermediate states, as it is shown in Section III.

C. Ordered structures in the density: superpositions of different L-subspaces

In this subsection, we consider ordered structures in GS's with no well defined angular momentum in two different situations. On the one hand, we build (somewhat *ad hoc*) linear

combinations of different Ψ_L's to explicitly reveal the structure present in the expectation value of the density operator. We obtain ordered IP's for combinations, whenever one of the contributing Ψ_L's has an ordered hidden IP contained in its pc function. On the other hand, after the introduction of an anisotropic term to the Hamiltonian which mimics the deformation introduced by the stirring laser, we perform numerical diagonalization without the restriction of angular momentum conservation, and obtain in this way GS structures with broken symmetry. These exact calculations give hints, how to construct approximated GS superpositions in the previous *ad hoc* construction.

To explain more precisely, how the first procedure works, we start from the pc function and observe what kind of ordered structures can be expected. In case of the Laughlin state $L = 20, N = 5$, the pc function suggests that the atoms form a pentagon. Quite generally, the best way to visualise this structure within the first procedure is to form a superposition $A\Psi_L + B\Psi_{L+N}$, where Ψ_L is the GS that contains a hidden ordered IP. It is easy to understand this result from what follows. The terms that contribute to the broken cylindrical symmetry are those of the form $\langle \Psi_L \mid a_i^\dagger a_j \mid \Psi_{L+M} \rangle$ with $M \geq 1$. However, it is necessary to arrive at $M = N$ in order to obtain contributions from all the sp states contained in Ψ_L. To be more precise, none of the combinations from $L = 20 + 21$ to $L = 20 + 24$ reproduces the structure of $L = 20$ for $N = 5$. It is necessary to combine $L = 20 + 25$ to obtain the regular pentagon implicit in Ψ_{20}. The best contrast is obtained for $A = B = 1$, and not for a small amount of Ψ_{L+N} as one would expect if only a perturbation would be necessary.

It is important to stress, that the ordered hidden IP was obtained in the Laughlin state $L = 20$ for $N = 5$. In order to assure that this state is the GS, a very small amount of kinetic energy is necessary in such a way that the states $L + M$ for $M \geq 0$ are quasi-degenerate. Then, the combination considered above corresponds to a "legitimate" GS.

The second procedure, followed in order to obtain ordered structures as, e.g., multiple vortex states, was suggested by experiments. In the experimental setup described by Chevy *et al.* [1] and by Madison *et al.* [10], vortices are generated as equilibrium states of a Bose condensate rotating under the action of a stirring laser that produces anisotropy in the XY plane. Subject to this anisotropic potential, the state with vortices is a GS, and it survives during the time of flight (TOF) detection as an excited state of the restored symmetric Hamiltonian after the trap is switched off.

With this idea in mind, we introduce an additional anisotropic term in the Hamiltonian given by $\hat{V}_p = A\sum_{i=1}^{N}(x^2-y^2)_i$ or in second quantized form as [48]

$$\hat{V}_p = \frac{A}{2}\lambda^2 \sum_m \left[\sqrt{m(m-1)}a_m^+ a_{m-2} + \sqrt{(m+1)(m+2)}a_m^\dagger a_{m+2}\right] \ . \tag{17}$$

We assume this term to be a small perturbation of the system, thus, $\frac{A\lambda^2/2}{\hbar(\omega_\perp-\Omega)} << 1$, and perform exact diagonalization to obtain the GS of $H+V_p$.

Amazingly, the structure of, say, two vortices can only be obtained at very specific plateau steps Ω_{cn}. There, the GS is a combination of quasi-degenerate Ψ_L-states which are coupled by a perturbing term slightly larger than their energy difference but much smaller than the next eigenenergy. As a consequence, the linear combination of the states above has nearly equal coefficients. Thus, a direct *ad hoc* combination of degenerated states of the symmetric Hamiltonian of Eq. (1) are educated guesses to reveal underlying structures. This combination was previously used by Wilkin *et al.* in exact diagonalization calculations to obtain two vortices [26]. More precisely, the unique situation where vortices are generated in the density corresponds to the steps in the L_{gs} dependence on Ω, where a degeneracy of states with different L takes place at Ω_{cn}. At first sight, this result does not agree with the experimental results reported by Chevy *et al.* [1]. However, it can be attributed to a essentially different behaviour of systems with a large and a small number of atoms, respectively. As N grows, the size of some of the plateaus shown in Fig. 1 drastically shrinks in such a way that finite ranges of Ω-values with energetically degenerate states become possible; not only at critical values Ω_{cn}. In Fig. 2, we show the appearance of such microplateaus obtained for $N = 6$, 7, 8, and 9.

Deduced from these features, our prediction is that the experimental graph, analogous to the one displayed by Chevy *et al.* [1] in their Fig. 2 which shows a monotonous growth of the vortex contribution to L_{gs} as a function of Ω, from the first vortex nucleation (at Ω_{c1}) to the turbulent regime, would look radically different for small N. We expect that it would present a curve with minima at those values of Ω where the GS is deep in a plateau, and exhibits no vortices in the density. Vortices will solely be visible on microplateaus surrounding Ω_{cn}. For fixed but larger N, the microplateaus contain more and more states as Ω increases, and thus a larger number of vortices is nucleated. Ultimately, in the large N limit, the number of vortices becomes proportional to the rotational frequency.

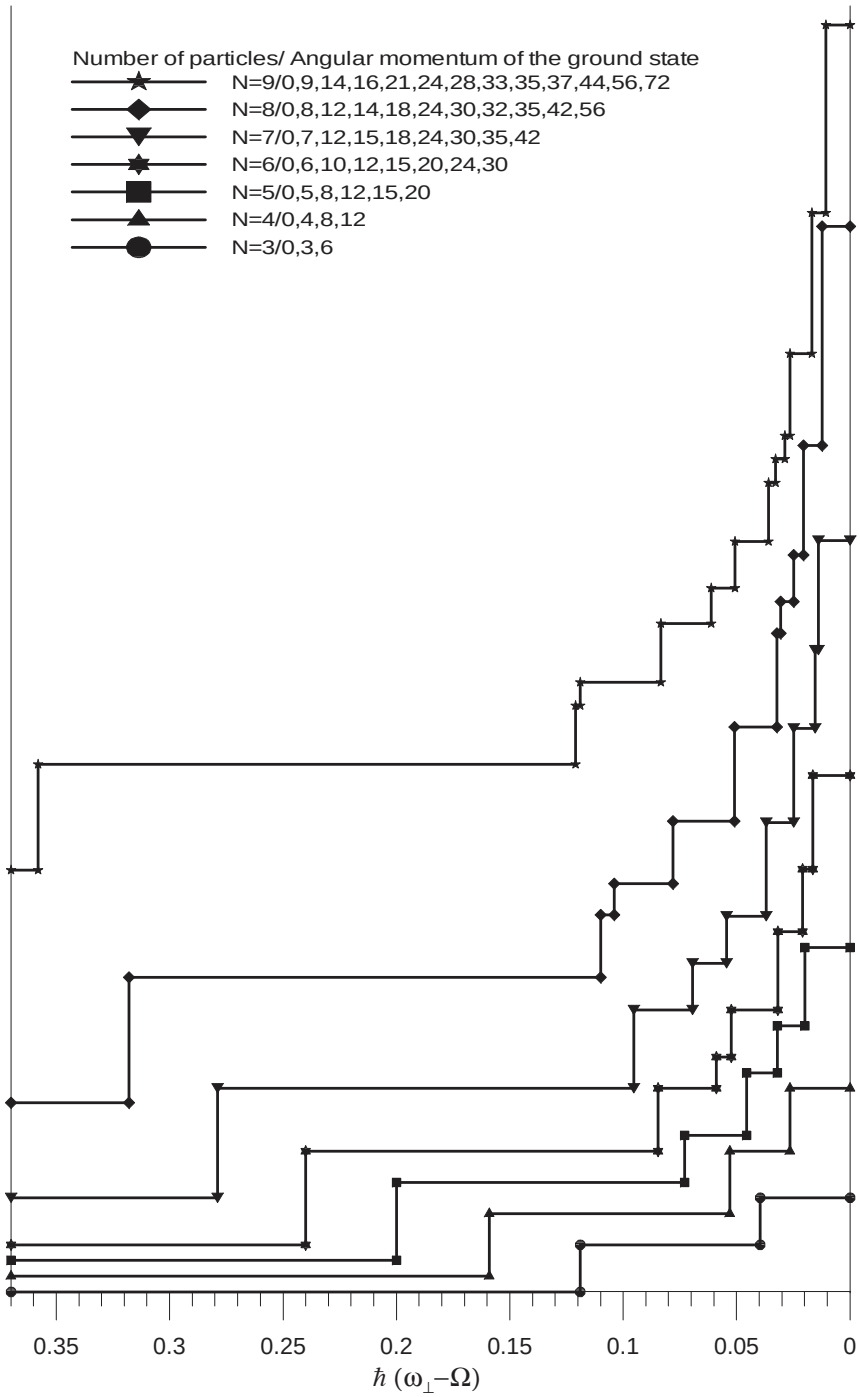

FIG. 2: The same as in Fig. 1 for $N = 3$ to 9 from bottom to top. Graphs are vertically shifted for clarity. The (quasi-)degenerate states within the same step are not included.

III. NUMERICAL RESULTS

In what follows, we display the results obtained from exact diagonalization for $g\lambda^2 = 1$ in units of $\hbar\omega_\perp$. The values $\omega_\perp = \Omega = 0$ were considered for density and correlation functions of single states, or combinations of states with well defined angular momentum, as the diagonalization of H depends only on the interaction energy. In contrast, specific values of α and β (see Eq. (3)) are considered when the diagonalization of $H + V_p$ is performed. Correlation functions are always displayed in pairs, a 3D and a contour plot, unless otherwise specified. We consider λ and $\hbar\omega_\perp$ as units of length and energy unless otherwise stated.

For $N \gg 1$, the first vortex is nucleated at $\Omega_{c1} = \omega_\perp - \frac{gN}{8\pi}$ when the transition from $L = 0$ to $L = N$ takes place at the first step of $L_{gs}(\Omega)$. The $L = N$ state whith a vortex at the centre is the GS from Ω_{c1} to Ω_{c2} (see Fig. 1). This state is characterized by a high occupancy of the $m = 1$ sp state and circular symmetry possessing no space correlations. In contrast, for small values of N a vortex is not clearly manifested unless a considerably large number of atoms is considered, as it is shown in Fig. 3, where the pc of the $L = N$ state is displayed for $N = 3$, 10 and 20. In all the cases, the density has a minimum at the origin and r_0 is set to its maximum. The slow tendency to recover the behaviour of large condensed systems is explained in Fig. 4, where the occupation of the $m = 1$ sp state over N is shown. Namely, for few atoms, the angular momentum of the state is not fully due to vortices. For a large number of atoms, Nakajima and Ueda have analyzed the formation of the first vortex, from its initial nucleation at the cloud boundary towards its final stabilization at the centre [49]; our results share some similarity with this situation: for small N, the vortex is not yet fully inside the trap, and as N increases, it approaches the trap centre from the boundary of the cloud.

In Fig.'s 5 to 9, we show the main results for $N = 3$ including the ground state evolution as Ω increases. Fig. 5a shows the lowest eigenenergies for each L, the so-called Yrast line. The initial points of the plateaus, at $L = 0, 3$ and 6 are the unique possible GS's (besides degeneracies at the steps). A general result is that the plateau previous to the Lauhglin state (from $L = 3$ to $L = 5$ in this case) has always N points. Fig. 5b is similar to Fig. 1 for $N = 5$. The densities from $L = 0$ to 9 are shown in Fig. 6. The parameter r_0 used in the pc calculation was set to the maximum of the density unless it is located at the centre. Then, $r_0 = 1$ is used if not stated elsewise. Fig.'s 7 and 8 display the pc function

for $L = 0, 3, 4, 5, 6$, and 9. The system evolves from a completely "condensed" system at $L = 0$ to the Laughlin state at $L = 6$ where a clear triangular structure appears. The loss of condensation is related to the increase of space correlations. To complete the analysis, we show in Fig. 9 the evolution of sp occupations, and demonstrate that "macroscopic" occupation of a specific sp wave function vanishes as L increases.

In order to see how the previous general tendency evolves as N increases, we analyzed the $N = 5$ case. In Fig. 10 we show the densities of the GS's from $L = 0$ to the Laughlin state, and in Fig.'s 11 and 12 we display their pc. The same tendency towards space ordering at the Laughlin state is clear. In addition, it can be inferred from the $L = 20$ case that correlations are stronger for nearest neighbours as a manifestation of partial long range order in finite systems. In Fig. 13 the occupations of sp states are shown. It is remarkable that some indications of the Laughlin state typical for large systems, i.e., a flat density at the central part and a hump at the edge are already manifested in such small systems, as it can be seen in the last graphs of Fig. 13 and Fig. 10, respectively. Moreover, the density at the origin is very close to $1/(2\pi)$, as necessary for a homogeneous system at filling factor 1/2.

In Fig.'s 14 and 15, we concentrate on the Laughlin state for $N = 3, 4, 5, 6, 7$, and 8 atoms. The left hand side picture for $N = 3, 4$ and 5 contains the pc function and the right hand side displays the density of the superposition made from L and $L + N$. This superposition of quasi-degenerated states becomes a possible realization of a GS for a certain value of Ω, as commented previously. The value of the parameter r_0 in the pc functions was obtained in a different way as the one used previously. Taking advantage of the fact that the Laughlin wave function (Eq. (6)) is the exact solution, and knowing that its pc shows a ring shape structure of an unknown radious r_0, we can maximize the probalibity distribution given by,

$$\mid \Psi_{Laughlin}(\vec{r_1}, \vec{r_2}, ...\vec{r_N}) \mid^2 = e^{-T} \tag{18}$$

where

$$T = \sum_i \frac{r_i^2}{2\lambda^2} - 2q \sum_{i<j} \ln \mid z_i - z_j \mid \tag{19}$$

(with $q = 2$ for the bosonic Laughlin state), or equivalently, minimize T with respect to r_0. Minimization yields $r_0 = \sqrt{N-1}$ (or $r_0 = \sqrt{N}$ if one atom is at the origin as for $N = 6$, 7 and 8) which is always smaller than the size of the system given by $R = \sqrt{4N-2}$. To see the evolution of these hidden ordered structures as N increases, the "degree of correlation"

C as a function of N is displayed in Fig. 16; C is defined as the height of the maximum peak in the pc function. It decreases for increasing N as it is expected in order to recover the quantum liquid character of the Laughlin state for large systems.

Finally, for $N = 5$ and 6, Fig. 17 shows patterns of two incipient vortices obtained from full diagonalization of $H + V_p$ at $\hbar(\omega_\perp - \Omega) = 0.0458$ and $\hbar(\omega_\perp - \Omega) = 0.05904$ in units of $\hbar\omega_\perp$, respectively. The possibility to obtain these patterns for the given anisotropy strongly depends on the possibility to obtain truly degenerate states with angular momenta L and $L \pm 2$ at one of the steps $L_{gs}(\Omega)$. For $N = 7$ we were not able to find such steps. For $N = 5$ the result of the diagonalization at the third step, where $L = 8, 10$ and 12 are involved, is that the weights of $L = 8$ and 10 within the expansion of the GS are much larger that the weight of $L = 12$. This leads in effect to a state with expected vortex angular momentum lower than 10, in agreement with the results demonstrated in Ref. [50] related to the fact that the contribution of a vortex to the total angular momentum depends on its distance from the origin, it runs from N at the centre to zero at the trap boundary.

IV. DISCUSSION AND SUMMARY

The main result of this paper is the identification of important differences between large and small systems of rapidly rotating cold bosonic atoms. These differences can be understood by looking at the expected values of the density and the pc functions, on which we have concentrated our analysis. The characterization of small samples in rotating traps has recently attracted increasing interest due to the possibility to deal with a few number of atoms per well in optical lattices [45].

Within the regime of low rotational frequency, we obtain that a relatively large number of atoms is necessary to nucleate the first vortex carrying N units of angular momentum. The evolution towards the condensed state with $L = N$ is shown by the increase of the occupation of the sp $m = 1$ state as N increases. On the other hand, in the regime of strong rotation, space correlations increase significantly, and in the Laughlin state a hidden ordered structure modulates the pc pattern. For small systems, the atoms sit around a ring of radius $r_0 = \sqrt{N-1}$ ($N = 3$, 4 and 5) or $r_0 = \sqrt{N}$ ($N = 6$, 7 and 8). The degree of correlation defined as the height of the peaks in the ordered pattern decreases with N, evolving towards

a non-correlated structure of a quantum liquid. We have argued about the observability of the ordered IP in similar experiments as those reported, for instance, by Fölling *et al.* [22].

Numerous references have analyzed the Wigner structures of few electrons [51, 52, 53, 54, 55, 56, 57], mostly for filling factors less than 1/3, and exhibited in the density (and not in the pc function). It is important to remark that it is well established from exact diagonalization studies in a torus geometry and from the analysis of the Laughlin wave function, that states of filling factor 1/3 for electrons and 1/2 for bosons are fermionic quantum liquids in the thermodynamic limit (cf. [58]). Whenever the Laughlin function is a good approximation, its implied properties are independent from the interaction. However, for small confined systems the previous results do not apply, and the analysis of some of their properties relies on the competition between the kinetic and interaction energies, aside from their statistics.

Suggested by our results, a possible explanation for the realization of Wigner molecules in the Laughlin states for few bosons is the following. The first observation is that the nature of the GS does not depend on the kinetic part as the diagonalization is fully determined by the interaction, in other words, the structure does not result from the competition between different kinds of energy. In addition, as the repulsive interaction energy is zero in the Laughlin state, it seems that the reason why the atoms choose symmetric and well separated positions is due to two conditions, firstly, the system must have a large angular momentum given by $L = N(N-1)$ (which means large distances from the origin) and secondly, each atom is surrounded by a quasihole (which leads to effective mutual repulsion). This last statement is supported by the following observation. The contour plots of $N = 3$ for $L = 4$ and $L = 5$ in Fig.'s 7 and 8 suggest that in those precursory states (the Laughlin state has $L = 6$), quasi-holes not attached to atoms are created without cost of internal energy, the contribution to the angular momentum of each one would evolve as 1/3 (in $L = 4$), 2/3 (in $L = 5$) and 3/3 until the Laughlin structure becomes possible with one quasi-hole attached to each atom, lowering the interaction energy. A final observation relates to the evolution of this behaviour as N increases. Due to the fact that the dependence of L on N is quadratic, the increase of L with N is more efficient for large N, and atoms do not have to be widely separated. Thus, the symmetric distribution tends to disappear. Recently, it has been proposed that the phenomenology of strongly correlated bosonic and fermionic rotating systems converges to te case of classical particles, and finally cristallizes at high

rotational frequencies [59]. Our results exhibit some traces of such cristallization, but it should be pointed out that this "cristallization" ceases to be manifested when the bulk structure starts to dominate the system. This happens for bigger particle numbers, where the GS at Laughlin angular momentum will start to behave more and more like a true quantum liquid as pointed out above.

Finally, precursors of two-vortex arrays are obtained as the ground states of an asymmetric Hamiltonian that models the experimental setup used to increase the angular momentum of a trapped Bose condensate by a stirring laser. We conclude that the possibility to nucleate vortex patters in the density is restricted for small N to the specific values Ω_{cn} at the steps where several degenerate or quasi-degenerate states of different angular momentum L coexist. This produces peaks in the vortex angular momentum dependence on Ω. We predict these peaks to broaden as N increases, due to the appearance of "microplateaus" which in turn lead to finite ranges of Ω values where quasi-degenerate states coexist.

We thank J. Dalibard, L. Pitaevskii, G.V. Shlyapnikov, and S. Stringari for fruitful discussions. We acknowledge support from the Deutsche Forschungsgemeinschaft (SFB 407, SPP 1116, GK 282, 436 POL), the EU Programme QUPRODIS, ESF PESC QUDEDIS, EU IP Programme "SCALA", and the MEC (Spanish Goverment) in terms of the contracts FIS2005-04627 and FIS2004-05639 and 2005SGR00343 from Generalitat de Catalunya.

---

[1] F. Chevy, K.W. Madison and J. Dalibard, Phys. Rev. Lett. **85**, 2223 (2000).

[2] M.H. Anderson, J.R. Ensher, M.R. Matthews, C.E. Wierman and E.A. Cornell, Science **169**, 198 (1995).

[3] K.B. Davis, M.-O. Mewes, M.R. Andrews, N.J. van Druten, D.S. Durfee, D.M. Kurn, and W. Ketterle, Phys. Rev. Lett. **75**, 3969 (1995).

[4] C.C. Bradley, C.A. Sackett, R.G. Hulet, Phys. Rev. Lett. **78**, 985 (1997); C.C. Bradley, C.A. Sackett, J.J. Tollett and R.G. Hulet, Phys. Rev. Lett. **75**, 1687 (1995).

[5] L. Pitaevskii and S. Stringari, *Bose-Einstein Condensation* (Oxford Sci. Pub., Oxford, 2003).

[6] M.R. Andrews, C.G. Townsend, H.J. Miesner, D.S. Durfee, D.M. Kurn and W. Ketterle, Science **275**, 637 (1997).

[7] Juha Javanainen and Sung Mi Yoo, Phys. Rev. Lett. **76**, 161 (1996); J. Javanainen and M. Wilkens, Phys. Rev. Lett. 78, 4675-4678 (1997).

[8] Y. Castin, J. Dalibard, Phys. Rev. A **55**, 4330; for a review see P. Villain, M. Lewenstein, R. Dum, Y. Castin, L. You, A. Imamoglu, and T.A.B. Kennedy, J. Mod. Optics **44**, 1775 (1997).

[9] J. Dziarmaga, Z.P. Karkuszewski, K. Sacha, Phys. Rev. B **36**, 1217 (2003).

[10] K.W. Madison, F. Chevy, W. Wohlleben and J. Dalibard, Phys. Rev. Lett. **84**, 806 (2000).

[11] J.R. Abo-Shaeer, C. Raman, J.M. Vogels, and W. Ketterle, Science **292**, 476 (2001).

[12] A. Abrikosov, Zh. Eks. Teor. Fiz. **32**, 1442 (1957), [Sov. Phys. JETP **5**, 1174 (1957)].

[13] In experiments of the ENS group, for instance, a laser beam forms a Gaussian optical potential. It rapidly oscillates through the trap centre along the direction that slowly rotates around the trap centre. Obviously, such a process couples states with various angular momenta.

[14] See for instance, G. Baym, Acta Phys. Pol. B **29**, 1839 (1998), and references therein.

[15] R.H. Brown and R.Q. Twiss, Nature **178**, 1046 (1956).

[16] M. Yasuda and F. Shimizu, Phys. Rev. Lett. **77**, 3090 (1996).

[17] M. Schellekens, R. Hoppeler, A. Perrin, J.V. Gomes, D. Boiron, A. Aspect, and C.I. Westbrook, Science **310**, 648 (2005).

[18] D. Hellweg, L. Cacciapuoti, M. Kottke, T. Schulte, K. Sengstock, W. Ertmer, and J. J. Arlt, Phys. Rev. Lett. **91**, 010406 (2003); L. Cacciapuoti, D. Hellweg, M. Kottke, T. Schulte, W. Ertmer, J. J. Arlt, K. Sengstock, L. Santos, and M. Lewenstein, Phys. Rev. A **68**, 053612 (2003)

[19] E. Altman, E. Demler and M.D. Lukin, Phys. Rev. A **70**, 013603 (2004).

[20] R. Bach and K. Rzążewski, Phys. Rev. Lett. **92**, 200401 (2004); R. Bach and K. Rzążewski, Phys. Rev. A **70**, 063622 (2004).

[21] Z. Hadzibabic, S. Stock, B. Battelier, V. Bretin and J. Dalibard, Phys. Rev. Lett. **93**, 180403 (2004).

[22] S. Fölling, F. Gerbier, A. Widera, O. Mandel, T. Gericke and I. Bloch, Nature **434**, 481 (2005).

[23] M. Greiner, C.A. Regal, J.T. Stewart, and D.S. Jin, Phys. Rev. Lett. **94**, 110401 (2005).

[24] D.M. Stamper-Kurn, A.P. Chikkatur, A. Görlitz, S. Inouye, S. Gupta, D.E. Pritchard, and W. Ketterle, Phys. Rev. Lett. **83**, 2876 (1999); J. Stenger, S. Inouye, A.P. Chikkatur, D.M. Stamper-Kurn, D.E. Pritchard, and W. Ketterle, Phys. Rev. Lett. **82**, 4569 (1999).

[25] R.B. Laughlin, Phys. Rev. Lett. **50**, 1395 (1983).

[26] N.K. Wilkin, J.M.F. Gunn, R.A. Smith, Phys. Rev. Lett. **80**, 2265 (1998); N.K. Wilkin and J.M.F. Gunn, Phys. Rev. Lett. **84**, 6 (2000).

[27] B. Paredes, P. Fedichev, J.I. Cirac, P. Zoller, Phys. Rev. Lett. **87**, 010402 (2001).

[28] R.E. Prange and S.M. Girvin, *The Quantum Hall Effect* (Springer-Verlag, Berlin 1990)

[29] N.R. Cooper, N.K. Wilkin, and J.M.F. Gunn, Phys. Rev. Lett. **87**, 120405 (2001); J. Sinova, C.B. Hanna, and A.H. MacDonald, Phys. Rev. Lett. **89**, 030403 (2002); N. Regnault and T. Jolicoeur, Phys. Rev. B **70**, 241307 (2004).

[30] N. Read and E. Rezayi, Phys. Rev. B **59**, 8084 (1999).

[31] G. Moore and N. Read, Nucl. Phys. B **360**, 362 (1991); M.A. Cazalilla, N. Barberan, and N.R. Cooper, Phys. Rev. A **71**, 121303 (2005).

[32] A.G. Morris and D.L. Feder, e-print cond-mat/0602037.

[33] I. Coddington, P. Engels, V. Schweikhard, and E.A. Cornell, Phys. Rev. Lett. **91**, 100402 (2004).

[34] V. Schweikhard, I. Coddington, P. Engels, S. Tung, and E.A. Cornell, Phys. Rev. Lett. **93**, 210403 (2004).

[35] V. Schweikhard, I. Coddington, P. Engels, V.P. Mogendorff, and E.A. Cornell, Phys. Rev. Lett. **92**, 040404 (2002); T.P. Simula, P. Engels, I. Coddington, V. Schweikhard, E.A. Cornell, and R.J. Ballagh, Phys. Rev. Lett. **94** 080404 (2005); S. Stock, B. Battelier, V. Bretin, Z. Hadzibabic, and J. Dalibard, Laser Phys. Lett. **2** (6), 275-284 (2005).

[36] M. Baranov, Ł. Dobrek, K. Góral, L. Santos, and M. Lewenstein, Phys. scr. **102**, 74 (2002).

[37] N.R. Cooper, E.H. Rezayi, and S.H. Simon, Phys. Rev. Lett. **95**, 200402 (2005).

[38] M.A. Baranov, K. Osterloh, and M. Lewenstein, Phys. Rev. Lett. **94**, 070404 (2005).

[39] J. Stuhler, A. Griesmaier, T. Koch, M. Fattori, T. Pfau, S. Giovanazzi, P. Pedri, and L. Santos, Phys. Rev. Lett. **95**, 150406 (2005).

[40] See e.g. special issue on ultracold polar molecules [Eur. Phys. J. D **31**, 149 (2004)].

[41] D. Jaksch and P. Zoller, New J. Phys. **5**, 56 (2003); E.J. Mueller, Phys. Rev. A **70**, 041603 (2004); A.S. Sorensen, E. Demler, and M.D. Lukin, Phys. Rev. Lett. **94**, 086803 (2005); K. Osterloh, M. Baig, L. Santos, P. Zoller, and M. Lewenstein, Phys. Rev. Lett. **95**, 010403 (2005).

[42] J. Ruseckas, G. Juzeliunas, P. Öhberg, and M. Fleischhauer, Phys. Rev. Lett. **95**, 010404

(2005).

[43] I. Bloch, private comm.

[44] G. Birkl, private communication; see also G. Birkl, F.B.J. Buchkremer, R. Dumke, and W. Ertmer, Opt. Commun. **191**, 1 (2001).

[45] M. Popp, B. Paredes, and J.I. Cirac, Phys. Rev. A **70**, 053612 (2004).

[46] M.A. Cazalilla, Phys. Rev. **A67**, 063613 (2003).

[47] L. Jacak, P. Hawrylak, and A. Wojs, *Quantum Dots* (Springer-Verlag, Berlin 1997).

[48] Such a model describes the experiments of Ref. [10] quite well, and has several different advantages: i) it has a simple analytical form and allows for simple calculations; ii) it also describes other kinds of "stirring", for instance, the one in which one uses an elliptical, rotating mask to generate the optical potential of Eq. (17).

[49] T. Nakajima and M. Ueda, Phys. Rev. Lett. **91**, 140401 (2003).

[50] F. Zambelli and S. Stringari, Phys. Rev. Lett. **81**, 1754 (1998).

[51] K. Jauregui, W. Häusler, and B. Kramer, Europhys. Lett. **24**, 581 (1993).

[52] K.Yang, F.D.M. Haldane, and E.H. Rezayi, Phys. Rev. B **64**, 081301 (2001).

[53] N. Shibata and D. Yoshioka, cond-mat/0308122.

[54] E. Rasanen, H. Saarikoski, M.J. Puska, and R.M. Nieminen, Phys. Rev. B **67**, 035326 (2003).

[55] C. Yannouleas and U. Landman, Phys. Rev. B **68**, 035326 (2003).

[56] C. Yannouleas and U. Landman, Phys. Rev. B **69**, 113306 (2004).

[57] B. Szafran, F.M. Peeters, S. Bednarek, T. Chwiej, and J. Adamowski, Phys. Rev. B **70**, 035401 (2004); B. Szafran, F.M. Peeters, S. Bednarek, T. Chwiej, and J. Adamowski, Phys. Rev. B **71**, 235305 (2005).

[58] D. Yoshioka,*The Quantum Hall Effect* (Springer-Verlag, Berlin 2002)

[59] S.M. Reimann, M. Koskinen, Y. Yu, M. Manninen, cond-mat/0602039.

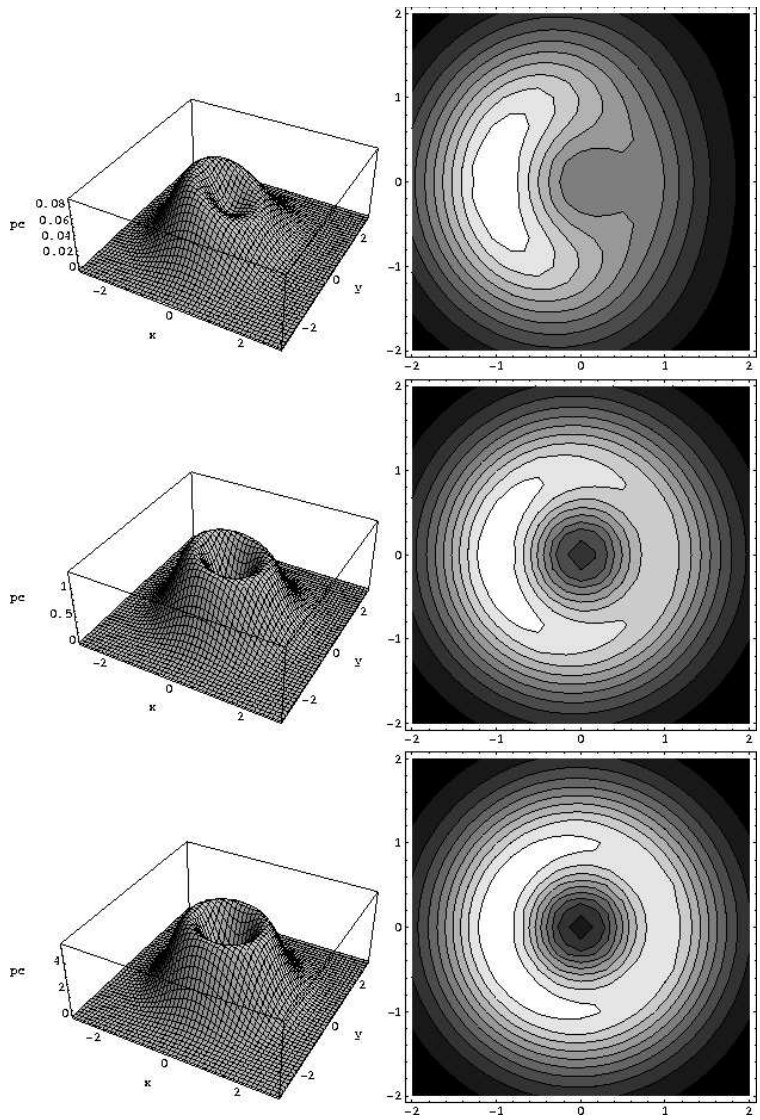

FIG. 3: Pair correlation function for $N = 3$, 10 and 20 of the $L = N$ state. The parameter $r0$ is equal to 0.8, 0.95 and 1.0 in units of λ respectively.

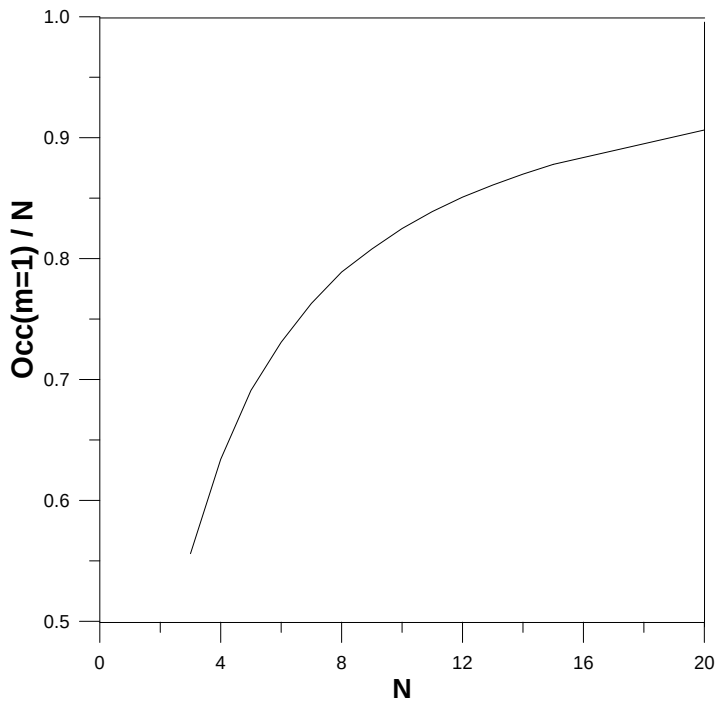

FIG. 4: Occupation of the m=1 single state divided by N as a function of N.

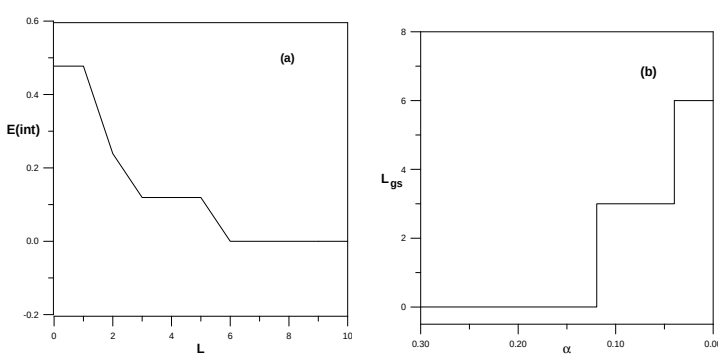

FIG. 5: For $N = 3$, a) interaction energy as a function of total angular momentum (Yrast line), b) angular momentum of the GS over α. The critical values for α at the steps are: 0.1194 and 0.0398 in units of $\hbar\omega_\perp$.

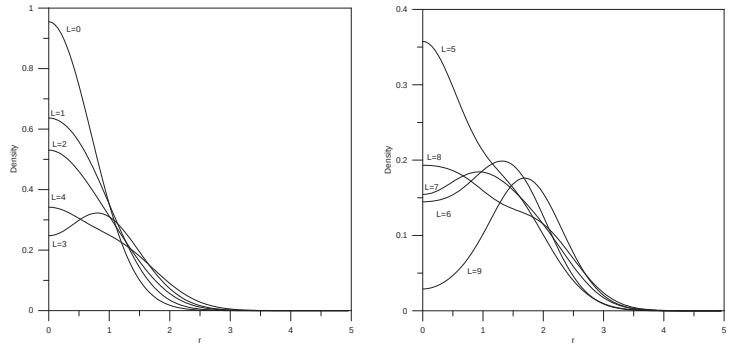

FIG. 6: N=3, density of the L-states

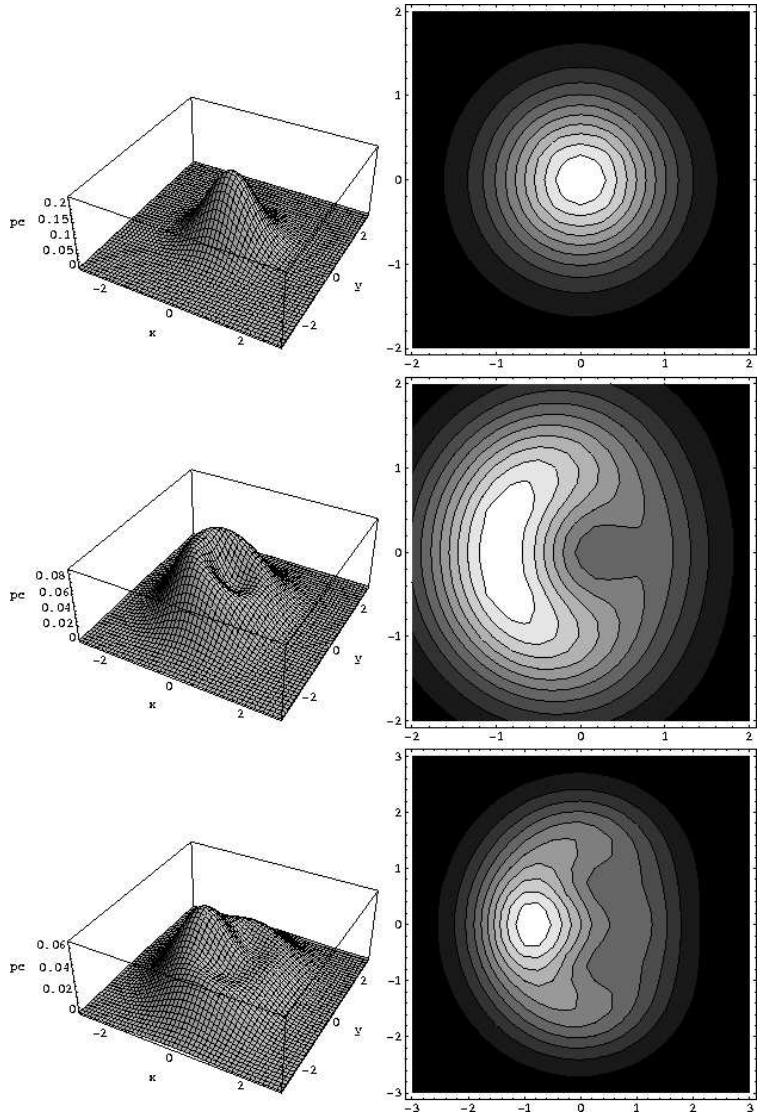

FIG. 7: Pair correlation function of $N = 3$, for $L = 0$, 3 and 4, $r0 = 1.0$, 0.8 and 1.0 respectively.

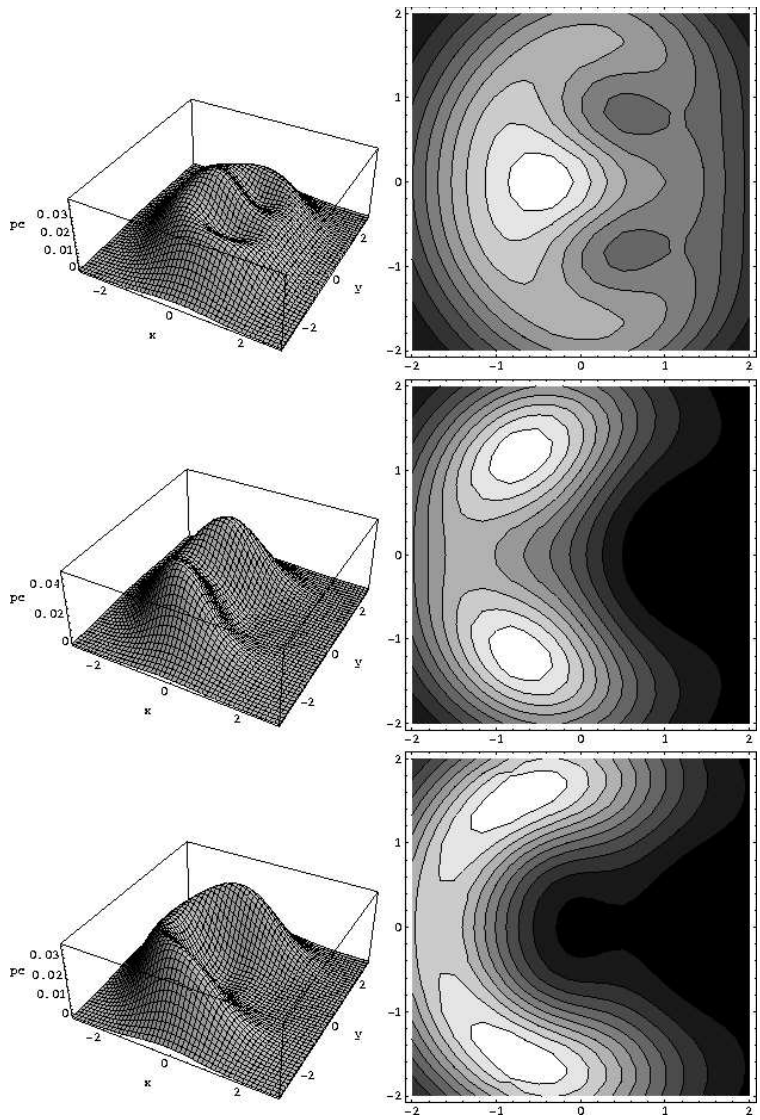

FIG. 8: The same as Fig.7 for $L = 5$, 6 and 9, $r0 = 1.0$, 1.3 and 1.7 respectively.

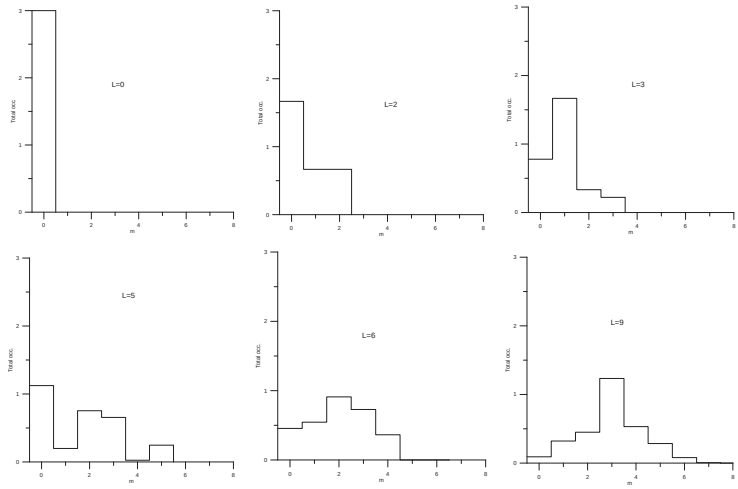

FIG. 9: For $N = 3$, total occupations of the single particle states of angular momentum m for several L-states.

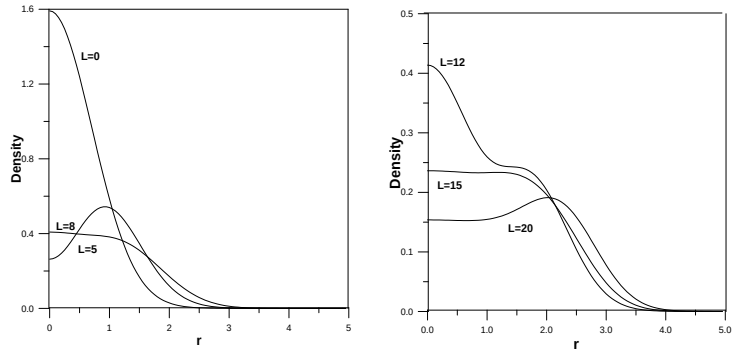

FIG. 10: N=5 density of the L-states (GS).

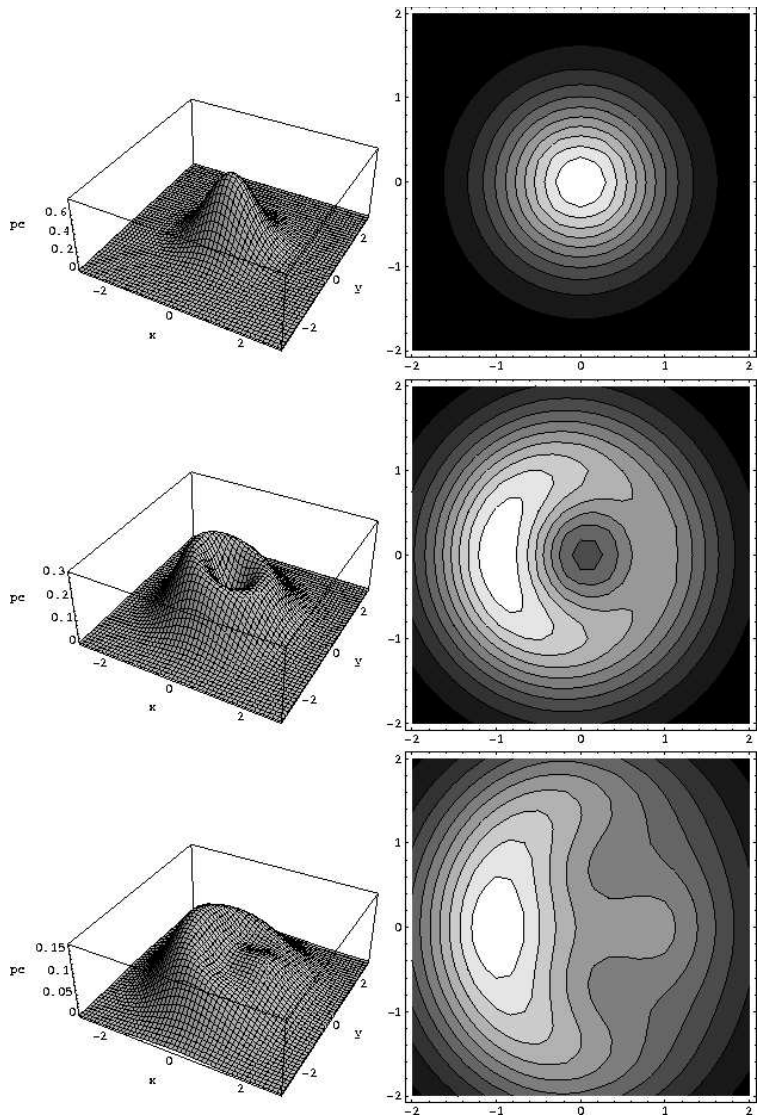

FIG. 11: Pair correlation of the L-states (GS) for $N = 5$ and $L = 0$, 5, and 8. $r0 = 1.0$, 0.9 and 1.0 respectively.

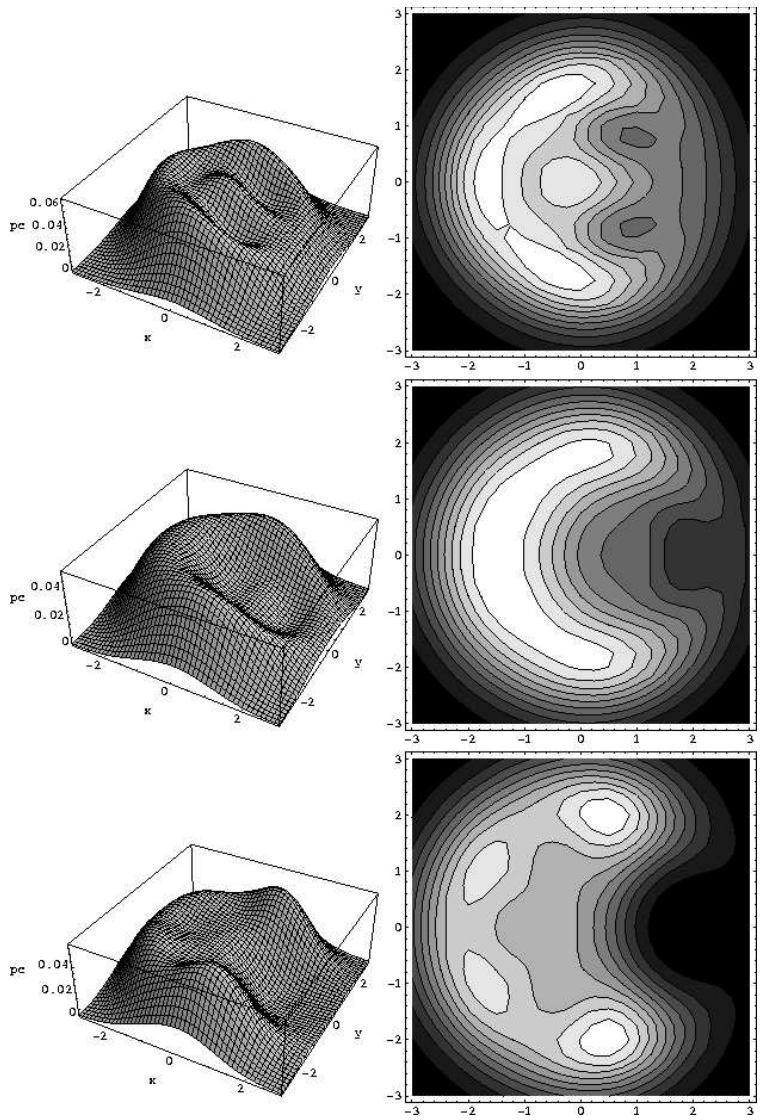

FIG. 12: Pir correlation of the L-states (GS) for $N = 5$ and $L = 12$, 15 and 20. $r0 = 1.0$, 1.0 and 2.0 respectively.

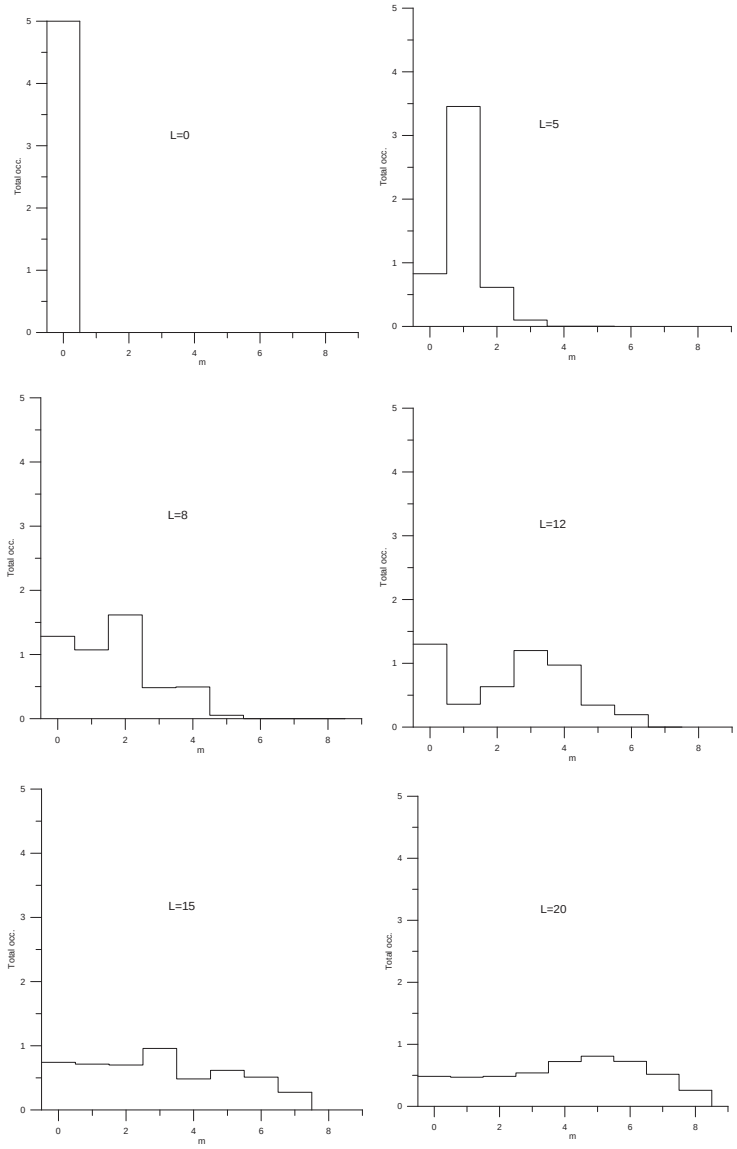

FIG. 13: N=5 occupations of the L-states (GS).

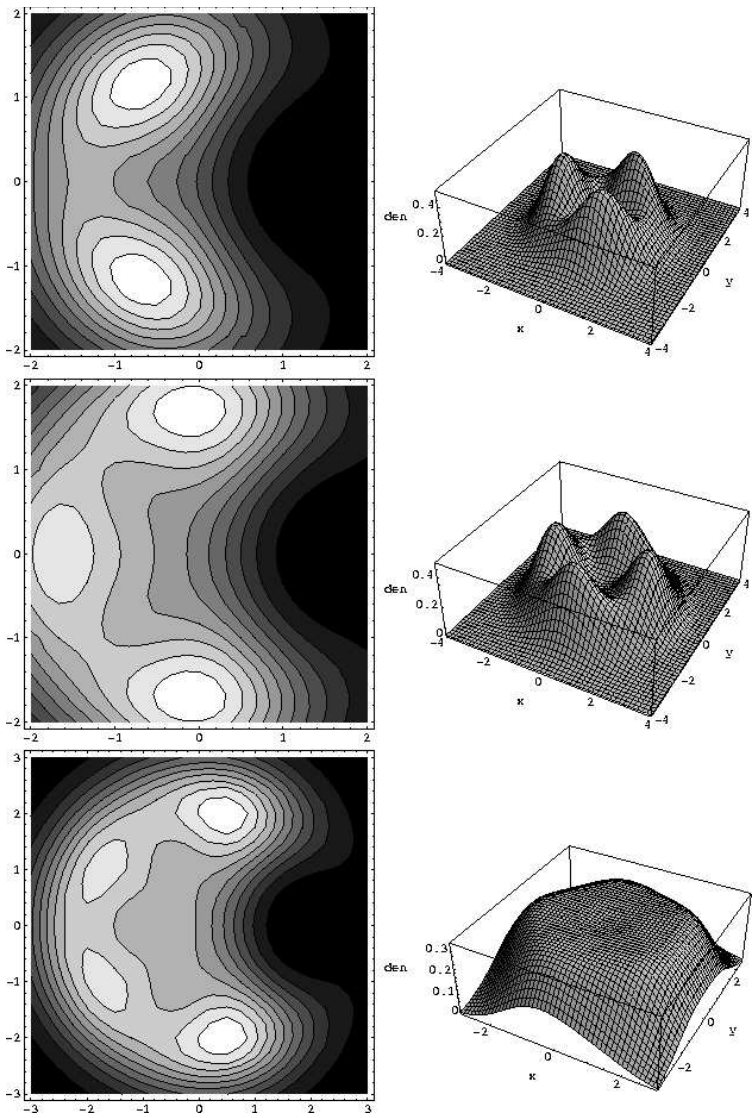

FIG. 14: For $N = 3$, 4 and 5 the left hand plots show the pair correlations (contour plots) for $L = 6$, 12 and 20 respectively (the Laughlin states), with $r0 = \sqrt{N-1}$. The right hand 3D-plots show the density of the mixtures (with equal coefficients) of angular momenta $6 + 9$, $12 + 16$ and $20 + 25$ respectively.

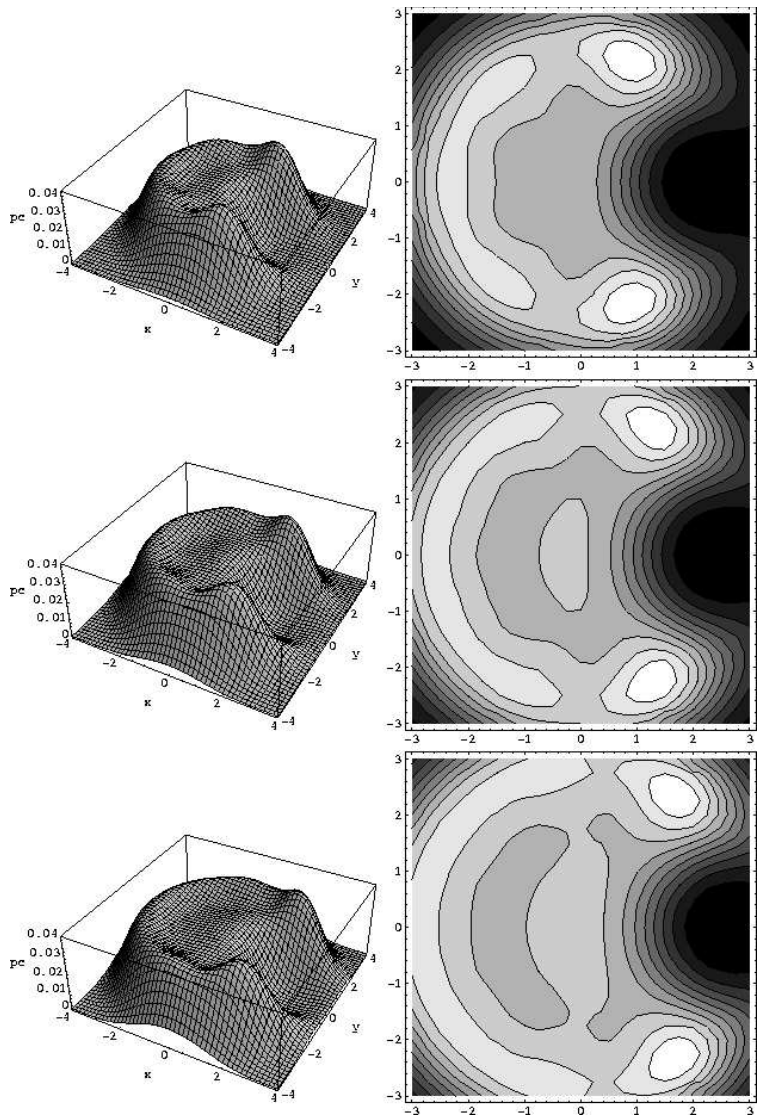

FIG. 15: For $N = 6$, 7 and 8 pair correlations (3D-plot and contour-plot) of $L = 30$, 42 and 56 respectively (the Laughlin states). We consider $r0 = \sqrt{N}$.

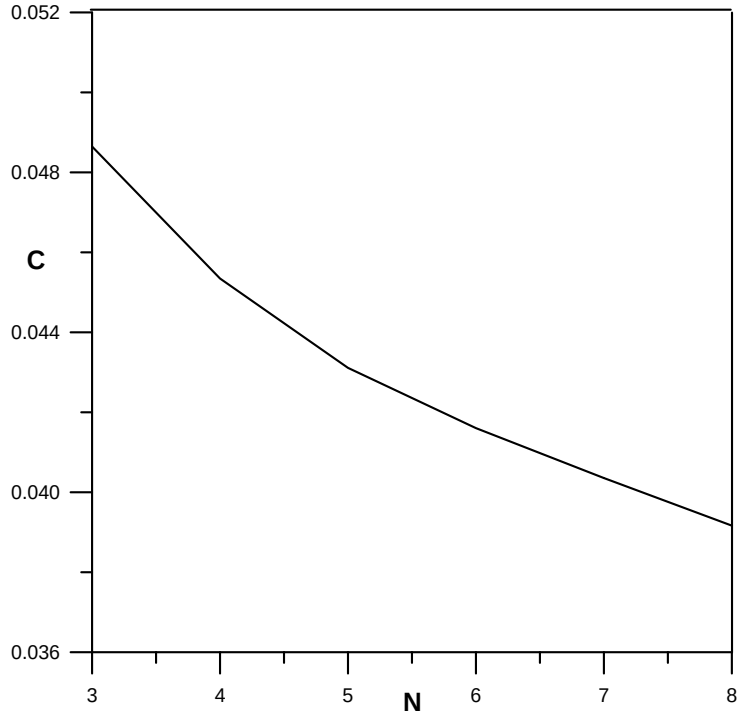

FIG. 16: Correlation degree (see text) of the Laughlin state as a function of N.

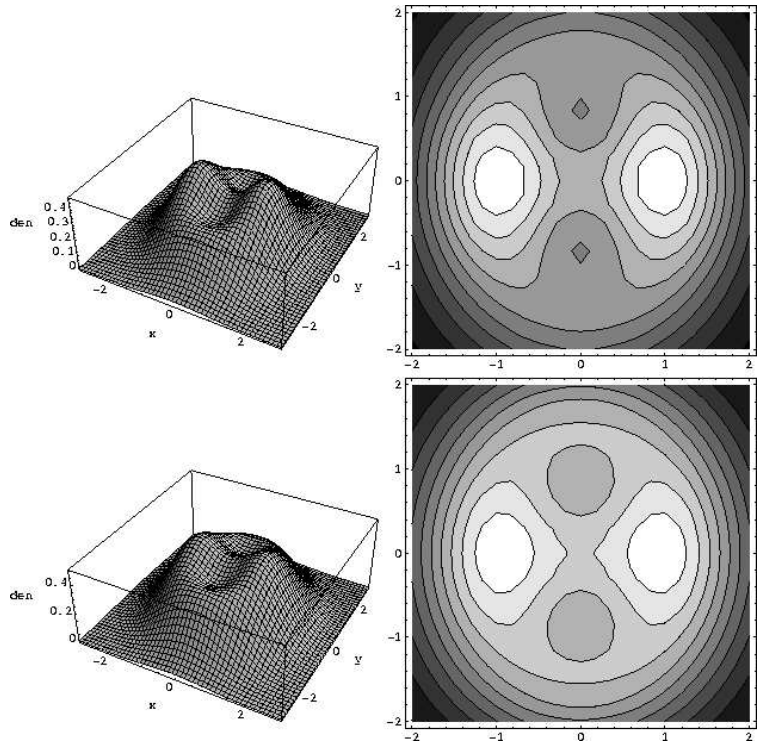

FIG. 17: For $N = 5$ and 6 density (3D-plot and contour-plot) of the two vortex structures. For $N = 5$, $L = 8 + 10 + 12$ and for $N = 6$, $L = 10 + 12 + 14$.